The effects of CdSe incorporation into bulk heterojunction solar cells†

Jilian Nei de Freitas,[a] Isabel R. Grova,[b] Leni C. Akcelrud,[b] Elif Arici,[c] N. Serdar Sariciftci[c] and Ana Flávia Nogueira*[a]

Received 28th January 2010, Accepted 18th March 2010
First published as an Advance Article on the web 30th April 2010
DOI: 10.1039/c0jm00191k

Hybrid solar cells based on CdSe nanoparticles and a PPV-type polymer containing fluorene and thiophene units (PFT) were investigated. The CdSe/PFT devices showed very low photocurrent and fill factor values, which was attributed to the poor charge transport in the TOPO-capped CdSe nanoparticle phase. Thus, ternary systems based on mixtures of PFT/CdSe and the fullerene derivative PCBM were investigated. The CdSe:PCBM ratio was varied, and nanoparticles with different sizes were also used. It was observed that for the optimized composition of 20 wt% PFT + 40 wt% CdSe + 40 wt% PCBM the devices presented higher photocurrents and efficiencies. The photophysical and electrochemical properties and microscopy images (AFM and HRTEM) of the ternary systems were systematically investigated to elucidate the mechanism of action of the inorganic nanoparticles in these ternary hybrid devices.

Introduction

Organic solar cells are among the most promising devices for cheap solar energy conversion. These devices are usually assembled with a mixture of a conjugated polymer and a fullerene derivative. The polymer acts as light absorber, electron donor and hole transporter while the fullerene acts as an electron acceptor and transporter. Hybrid solar cells assembled with the substitution of fullerenes with inorganic semiconductor nanoparticles, such as TiO_2, ZnO, $CuInS_2$, PbSe, CdSe and CdTe, have also been investigated as promising alternatives.[1–3] The use of inorganic nanoparticles has some advantages, related to the versatility of these materials, which often can be easily synthesized in a great variety of sizes and shapes, according to the desired properties.

One of the most used materials in hybrid solar cells are CdSe nanoparticles. In 2002, Huynh *et al.*[4] reported devices based on the combination of CdSe nanospheres or nanorods with poly(3-hexylthiophene) (P3HT), with power conversion efficiencies of up to 1.7%. Later, it was found that by optimizing the solvent used during film deposition, even higher efficiencies could be obtained.[5] Other CdSe structures, such as spherical nanoparticles crystallized in the zinc blend structure,[6] tetrapods[7,8] and hyperbranched nanocrystals[9] have also been used in combination with P3HT or poly[2-methoxy-5-(3,7-dimethyloctyloxy)-*p*-phenylene vinylene] (MDMO-PPV), resulting in devices with efficiencies around 1–2%. In 2005, Sun *et al.*[10] used CdSe tetrapods in combination with P3HT and the films prepared from 1,2,4-trichlorobenzene solutions resulted in devices with efficiencies of 2.8%, which is among the highest values reported for this kind of device. On the other hand, other attempts to make hybrid solar cells with CdSe resulted in low efficiency devices (much less than 1%).[11,12] As a general trend, the reported photocurrent and efficiencies vary significantly. This arises from some problems inherent to the nanoparticle/polymer systems, such as phase separation and poor dispersion properties of nanoparticles in the solvent, especially for 1-dimensional materials, such as nanorods and nanowires. The presence of capping molecules on the nanoparticle surfaces, especially when the thickness of the capping layer is high, can also hinder the charge transfer or charge transport processes. All these parameters are crucial because they affect both the operation and the reproducibility of the devices.

In this work, we propose a ternary hybrid system for application in organic solar cells, based on the incorporation of CdSe nanoparticles in a mixture of a polymer and [6,6]-phenyl C_{61}-butyric acid methyl ester (PCBM). The devices are fully characterized and the role of CdSe nanoparticles in the ternary system is carefully investigated and discussed.

Experimental

Materials

The characterization of the polymer used, poly(9,9-*n*-dihexyl-2,7-fluorenilenevinylene-*alt*-2,5-thienylenevinylene) (PFT), will be published elsewhere.[13] This material is an alternating copolymer with molar mass of ~7700 g mol^{-1} and maximum absorption wavelength at 430 nm. PCBM was purchased from Solenne BV (The Netherlands). All the materials were used as received.

Synthesis of CdSe nanoparticles

CdSe nanoparticles were synthesized according to the procedure of Peng *et al.*[14] Briefly, CdO (0.11 g, 0.89 mmol), tetradecylphosphonic acid (TDPA) (0.43 g 0.15 mmol) and trioctylphosphine oxide (TOPO) (7 g) were loaded into the reaction

[a]*Laboratório de Nanotecnologia e Energia Solar (LNES) – Universidade Estadual de Campinas, UNICAMP, P.O. Box 6154, 13083-970 Campinas, SP, Brazil. E-mail: anaflavia@iqm.unicamp.br; Fax: +55 19 35213023; Tel: +55 19 35213029*
[b]*Laboratório de Polímeros Paulo Scarpa (LaPPS) – Universidade Federal do Paraná, UFPR, Curitiba, Brazil*
[c]*Linz Institute for Organic Solar Cells (LIOS) – Johannes Kepler University Linz, Altenberger Strasse 69, A-4040 Linz, Austria*
† Electronic supplementary information (ESI) available: Table S1–2 and Fig. S1–S5. See DOI: 10.1039/c0jm00191k

flask and heated to 120 °C under argon and degassed for 20 min. Then, the mixture was heated to 340 °C, and the solution became clear. The temperature was lowered to 260 °C and the stock selenium solution (1 mmol of Se dissolved in 5 mL of trioctylphosphine) was quickly injected. The mixture was kept at 260 °C for 3 min or 6 h (nanoparticles with 2.0 or 3.0 nm of preferential diameter, respectively, as estimated from the optical band gap). An alternative procedure consisted of the injection of the Se precursor at 340 °C, keeping the reaction medium at this temperature for 2 h, which resulted in larger nanoparticles (4.0 nm of preferential diameter, as estimated from the optical band gap). The mixture was then cooled down quickly by a flow of air to the flask wall. The CdSe nanoparticles were isolated by precipitation with ethanol, re-dissolving with toluene, and re-precipitating with ethanol. This procedure was repeated several times to ensure the removal of excess amounts of surfactants and impurities.

Preparation of nanocomposites

Nanocomposites consisting of PFT/CdSe, PFT/PCBM or the ternary system PFT/CdSe/PCBM were obtained by preparing a toluene solution containing a fixed amount of polymer (5 mg mL^{-1}) and 80 wt% of CdSe and/or PCBM, where the CdSe:PCBM ratio was varied. Films of these nanocomposites were obtained by spin-casting the solutions (800 rpm, 40 s) resulting in films with thicknesses of ~90–120 nm.

Characterization

UV–Vis spectra were measured with a Cary 3G UV–Visibile Spectrophotometer and fluorescence spectra with an ISS Photon Counting Spectrofluorometer (excitation = 370 nm). Cyclic voltammetry was carried out in a conventional three-electrode cell (electrolyte: 0.1 mol L^{-1} of tetrabutylammonium tetrafluoroborate in anhydrous acetonitrile) with Ag/AgCl as reference electrode, a platinum wire as counter electrode and a polymer-coated platinum substrate (1 cm^2) as working electrode. Cyclic voltammograms were recorded at 30 mV s^{-1}, under nitrogen atmosphere, using an Eco Chemie Autolab PGSTAT 10 potentiostat. Film thickness and morphology were determined using a Veeco Nanoscope DI 3100 AFM microscope operating in tapping mode. The nanocomposites were analyzed using high-resolution transmission electron microscopy (HRTEM) in a HRTEM-JEM 3010 URP microscope operating at 300 kV. The samples were prepared by casting one drop of a toluene solution of CdSe nanoparticles, CdSe/polymer or CdSe/polymer/PCBM mixtures onto a copper grid support (300 mesh), previously covered with a layer of thin carbon film.

Solar cells

Bulk-heterojunction solar cells were prepared according to the following procedure: indium tin oxide (ITO) coated glass substrates were cut to square pieces 1.5 cm × 1.5 cm and approximately half of the ITO was chemically etched away. Substrates were then washed in an ultrasonic bath using acetone, isopropanol, ethanol and Millipore water for 30 min and dried under a nitrogen flow. A thin layer of poly(3,4-ethylenedioxythiophene)–poly(styrenesulfonate) (PEDOT:PSS) in aqueous solution (Baytron PH) was spin-coated onto the substrates using 15 000 rpm spin-coater speed, originating films of ~60 nm. Substrates covered with PEDOT were annealed on a hot plate for 10 min at 150 °C in air. The photoactive layer, consisting of polymer/PCBM, polymer/CdSe or the ternary mixture polymer/PCBM/CdSe, was spin-coated on top from chlorobenzene solutions, using 800 rpm for 40 s, with typical thicknesses of 100–120 nm. The films were dried for 20 min under vacuum. To finalize the preparation of the solar cells, a top electrode consisting of 0.7 nm LiF and subsequently 70 nm Al was evaporated under vacuum (~10^{-6} mbar). The size of the active area of the solar cells was ~10 mm^2. During all measurements the samples were kept at room temperature. Later, the devices were thermally annealed on a hot plate at 130 °C for 10 min under a nitrogen atmosphere and measured again.

A KHS Steuernagel solar simulator adjusted to give 100 mW cm^{-2} of AM1.5G irradiation by using a calibrated Si photodiode was used to illuminate the solar cells to determine the photovoltaic performance. Current–voltage curves were measured with a Keithley 236 sourcemeter in the dark and under illumination. The external quantum efficiency spectra were determined by shining light from a 75 W Xe lamp through an Acton monochromator and a chopper and measuring the resulting short-circuit current with an EG&G lock-in amplifier. All electrical measurements were made in a nitrogen glovebox to minimize degradation.

Results and discussions

X-Ray diffraction analysis showed that the synthesized CdSe nanoparticles have crystallized in the wurtzite structure (data not shown). Fig. 1 displays the absorption and emission characteristics and HRTEM images for nanoparticles synthesized varying the time and/or temperature during the synthesis. From the absorption spectra, it is possible to estimate the preferential diameter size in the sample, using the equation proposed by Yu *et al.*[15] (eqn (1)), where D_a is the preferential diameter size and λ_{max} is the maximum wavelength for the lowest energy excitonic absorption band. Using this method, the estimated diameters for the synthesized CdSe nanoparticles were 2.0 nm, 3.0 nm and 4.0 nm. Fig. 1 also presents the histograms, showing the size distribution of these materials, determined from HRTEM images, and the structure of the materials used in this work. The comparison of the diameters values obtained from absorption of HRTEM measurements for nanoparticles synthesized at different conditions can be found in Table S1 in the ESI.†

$$D_a = (1.6122 \times 10^{-9})\lambda_{max}^4 - (2.6575 \times 10^{-6})\lambda_{max}^3 + (1.6242 \times 10^{-3})\lambda_{max}^2 - (0.4277)\lambda_{max} + 41.57 \quad (1)$$

Fig. 2 presents the current–voltage (J–V) characteristics for photovoltaic cells assembled with the mixture of PFT with 80 wt% of CdSe with different sizes. For polymer/CdSe mixtures, the best photovoltaic responses are obtained when 60 to 90 wt% of nanoparticles are incorporated into the polymer matrix.[9,11,12,16] In this work, an intermediate amount of 80 wt% of CdSe was chosen. The absorption spectrum of PFT is shown in the inset in Fig. 2.

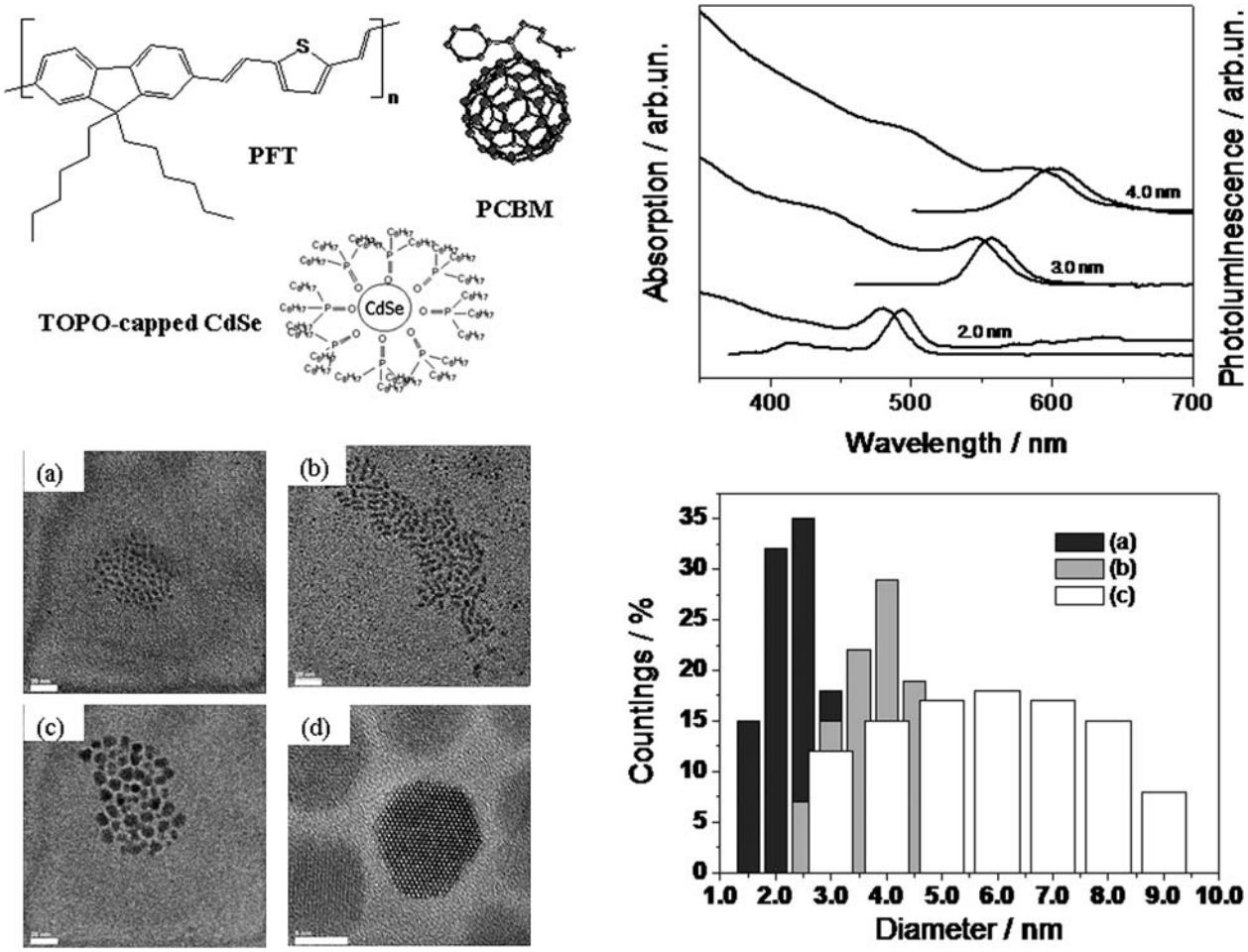

Fig. 1 Structure of the materials used in this work: polymer PFT, the fullerene derivative PCBM and CdSe nanoparticles covered with trioctylphosphine oxide (TOPO). Absorption and emission spectra for the CdSe nanoparticles synthesized with different preferential diameters and HRTEM images for materials exhibiting preferential diameter of (a) 2.0 nm, (b) 3.0 nm and (c,d) 4.0 nm, as estimated using eqn (1). The scale bar indicates (a,b,c) 20 nm or (d) 5 nm. For these images, the measured nanoparticles diameters were (a) 1.5–3.0, (b) 2.6–4.8 and (c) 3.2–9.0 as shown in the histograms. The histograms were obtained by measuring the diameter of 30 nanoparticles randomly chosen from HRTEM images.

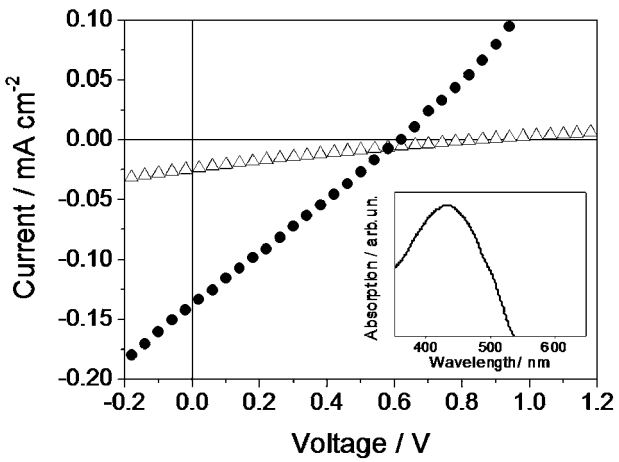

Fig. 2 *J–V* curves for photovoltaic cells illuminated at 100 mW cm^{-2} (active area ~0.1 cm^2), assembled with PFT and CdSe nanoparticles (80 wt%) with different sizes: (△) 2.0 nm or (●) 4.0 nm. The inset shows the absorption spectra of a film of PFT.

An interesting feature of the *J–V* curves in Fig. 2 is that there is an increase in short-circuit current (J_{sc}) when the nanoparticles size is increased from 2.0 to 4.0 nm. In principle, this enhancement in J_{sc} could be attributed to an improvement in light-harvesting in the solar cell assembled with larger CdSe nanoparticles, since their absorption is more extended into the visible region. It would be expected that the use of larger nanoparticles could lead to better light harvesting, thus contributing to the formation of more excitons, which would result in the formation of more free charges and, therefore, increase J_{sc}. On the other hand, the improvement in J_{sc} might also arise from a morphological effect. For the same concentration of CdSe nanoparticles dispersed in a polymer matrix, a percolation network is more easily formed in the case of larger nanoparticles.[17] Thus, the morphological effect would allow a better charge transport, also contributing to improved J_{sc} values. Additionally, the smaller the quantum dots, the higher the destructive effect of surface defects on the charge transport properties.

The open circuit voltage (V_{oc}) values obtained are very high: $V_{oc} \approx 0.6$ and 0.8 V for the devices assembled with CdSe with 4.0 or 2.0 nm of size, respectively. For this kind of device, V_{oc} is

dependent on the energetic difference between the HOMO of the polymer (−5.4 eV for PFT), and the LUMO of the electron acceptor material.[18] This difference in V_{oc} is probably related to the difference in the LUMO level energy presented by the nanoparticles with different sizes (LUMO is −3.1 and −3.6 eV for CdSe with 2.0 and 4.0 nm, respectively; see Table S2 in the ESI† for more details about energy levels for different CdSe nanoparticles).

Despite the high V_{oc} values and the improvement of J_{sc} upon addition of larger CdSe nanoparticles, the overall current values for both systems are very low ($J_{sc} \approx 50$ and 150 μA cm^{-2}). Also the fill factor (FF) values are low (FF < 25%), indicating a poor diode behavior for these systems. This suggests that the series resistance is very high and the shunt resistance is very small, caused by poor electric contacts at the interfaces and losses by recombination during charge transport, respectively. All these effects might be caused by a poor interaction between the polymer and CdSe, with the formation of phase separation and rough and/or heterogeneous morphologies or by a poor charge transfer process and/or poor charge transport.

The absorption and emission spectra of the polymer after addition of different amounts of CdSe were measured, showing a quenching of the PFT emission in the presence of the nanoparticles, as can be seen in Fig. S2 in the ESI.† Previously published works also show the quenching of polymer emission by the interaction with CdSe nanoparticles, and this may be considered as a first indication of the existence of charge transfer between these materials, either by the injection of electrons (from the polymer to CdSe) or by injection of holes (from CdSe to the polymer).[19–23] Some authors used the combination of other techniques, such as transient spectroscopy[19,20] to prove that efficient charge injection processes occur between inorganic nanoparticles and conjugated polymers. The polymer structure (especially concerning the presence of bulky ramifications), and the nature of the surfactant molecules on the nanoparticles surface seem to play a major role in the effectiveness of the photoinduced charge transfer processes in these hybrid systems.[22] In this work, TOPO-capped nanoparticles were used. It is accepted that the presence of TOPO hinders efficient charge transfer and may also prevent charge transport through hopping in the nanoparticles phase (inter-particles charge transport).[17] Phase separation is another phenomenon frequently observed in polymer–nanoparticle hybrid systems, and may lead to the formation of a nanomorphology where the nanoparticles are organized in "islands", dispersed in the polymer "sea", and this also causes poor charge transport in the CdSe phase.[17]

Considering the quenching of polymer emission observed after addition of CdSe nanoparticles, we believe that the inefficient inter-particles charge transport (hopping in CdSe phase) is more likely to cause the low FF and J_{sc} values observed in Fig. 2.

Since systems based on mixtures of conjugated polymers and CdSe have been widely used, we chose to investigate a new system, based on the combination of three components: polymer, CdSe nanoparticles and PCBM. In a two-component hybrid system, the nanoparticles must act as electron acceptors and transport these charges to the electrode. In a ternary system, it is expected that PCBM acts as the electron transport layer, and the CdSe nanoparticles may act only as sensitizers, contributing to increased light-harvesting and therefore generating more charges, but not necessarily transporting them.

CdSe has been widely used as a sensitizer in combination with TiO_2 in dye-sensitized solar cells.[24–27] In organic solar cells based on polymer/PCBM mixtures, the incorporation of metallic nanoparticles as a buffer layer to explore the plasmonic contribution has been widely investigated.[28–32] On the other hand, studies of ternary systems including polymer, PCBM and inorganic nanoparticles mixed as bulk heterojunctions have been much less explored.[33–36] Park *et al.*[34] incorporated small gold nanoparticle contents into a mixture of P3HT/PCBM. The authors reported an increase in J_{sc}, which was attributed to a better hole transport/injection in the ITO electrode, facilitated by the presence of the nanoparticles. Chen *et al.*[36] recently incorporated CdTe nanoparticles in the system P3HT/PCBM. After the annealing of the films, the authors suggested that the observed photoconductive gain under reverse bias was due to the formation of a surface layer rich in CdTe, which facilitated the injection of holes from the electrode to the polymer film. Both works show interesting features of organic–inorganic hybrid ternary systems.

Fig. 3a shows the J–V characteristics for solar cells assembled with PFT, CdSe (4.0 nm) and/or PCBM, with different ratios between the inorganic nanoparticles and the fullerene derivative. Three devices of each kind were measured, where each of them consisted of four different electric contacts. Thus, the values reported in Table 1 show the means and standard deviations obtained after 12 measurements. The deviation values are included because they indicate the reproducibility of the devices. The parameters extracted from these curves are listed in Table 1.

For all of the systems based on the ternary mixtures, the solar cells show a diode behavior, as well as high V_{oc} and J_{sc} values, independent of the CdSe : PCBM ratio. The overall FF values, although higher than that observed for the two-component based solar cells, are still rather low (~30%). This might be related to the poor light-absorption and limited charge transport observed for the polymer used (absorption maximum at 430 nm, and hole mobility ~10^{-6} cm^2 V^{-1} s^{-1} for PFT).[13]

The amount of CdSe incorporated into the system influences both V_{oc} and J_{sc}. As can be seen in Table 1, the higher the amount of CdSe, the higher the V_{oc} value. The fact that V_{oc} is sensitive to the presence of CdSe nanoparticles indicates that the new interface created after addition of this material is effective, and probably contributes somehow to the charge generation processes.

The concentration of CdSe in the ternary mixtures also affects J_{sc}. There seems to be an optimum condition (CdSe : PCBM 1 : 1 wt% ratio) at which J_{sc} is much higher. Considering that the TOPO-capped CdSe used has poor charge transport ability, as discussed before, the improvement in J_{sc} for a specific condition/concentration of materials could be explained by the following: the increase in CdSe content leads to an increase in light absorption (more excitons are generated and split, since CdSe is expected to inject charges into PCBM); on the other hand, the decrease in PCBM concentration damages the electron transport to the aluminium electrode. Therefore, there is a compromise between the generation of more charges and their effective transport, reflected by the optimum concentration of CdSe and PCBM in the active layer. Chen *et al.*[36] reported an increase in photoconductive gain under reverse bias after incorporation of CdTe nanoparticles into P3HT/PCBM/CdTe devices. However,

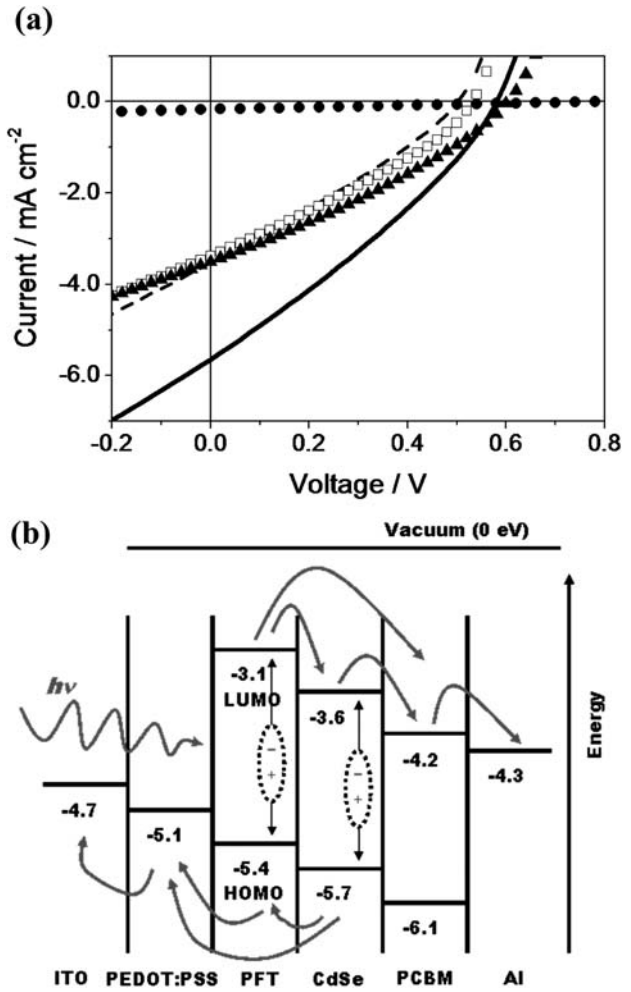

Fig. 3 *J–V* curves (a) for photovoltaic cells illuminated at 100 mW cm^{-2} (active area ~0.1 cm^2), assembled with 20 wt% of PFT, and 80 wt% of PCBM and/or CdSe (4.0 nm), with different concentrations: (---) 1 : 0, (□) 0.7 : 0.3, (—) 1 : 1 (▲) 0.3 : 0.7 and (●) 0 : 1 wt% PCBM : CdSe ratios. Schematic diagram (b) of the energy levels of in the ternary system solar cell showing the HOMO and LUMO levels of the materials and work function of the electrodes. The arrows indicate the expected charge transfer and charge transport processes.

Table 1 Photovoltaic parameters obtained for solar cells assembled with PFT and CdSe and/or PCBM with different concentrations (active area ~0.1 cm^2), illuminated under 100 mW cm^{-2}: short-circuit current (J_{sc}), open circuit voltage (V_{oc}) and fill factor (FF). The values presented correspond to the means and standard deviations after 12 measurements

PCBM : CdSe (wt% ratio)	J_{sc} (mA cm^{-2})	V_{oc} (V)	FF (%)	η (%)
1 : 0	3.5 ± 0.3	0.48 ± 0.03	28 ± 1	0.48 ± 0.04
0.7 : 0.3	3.2 ± 0.2	0.53 ± 0.01	30 ± 1	0.52 ± 0.03
1 : 1	4.5 ± 0.4	0.57 ± 0.02	30 ± 1	0.76 ± 0.06
0.3 : 0.7	3.7 ± 0.3	0.60 ± 0.01	31 ± 1	0.62 ± 0.03
0 : 1	0.16 ± 0.02	0.90 ± 0.10	22 ± 2	0.03 ± 0.00

under forward bias, in the region where the photovoltaic properties of solar cells are evaluated, the authors observed the suppression of current after mixing with the inorganic nanoparticles.

Fig. 3b displays a schematic diagram of the energy levels of the ternary component-based solar cells, and the charge transfer/transport processes expected for these devices: upon incidence of light, both PFT and CdSe might absorb photons and generate excitons, which might result in electron transfer from the polymer to CdSe or PCBM, and from CdSe to PCBM, or hole injections from CdSe to the polymer. The hole transport is accomplished by the polymer, while the electrons are transported in the PCBM phase. The ability of TOPO-capped CdSe nanoparticles to absorb light and inject electrons in C_{60} has been shown by Biebersdorf *et al.*,[37] and corroborates the mechanism proposed here.

Fig. 4 shows the IPCE (incident photon to current efficiency) of solar cells. In Fig. 4a it can be seen that the maximum efficiency is reached for the ternary system assembled with 1 : 1 wt% CdSe : PCBM ratio. All curves have a peak in the IPCE around 450–500 nm, which is the same region where the polymer absorption is maximum. The CdSe characteristic absorption

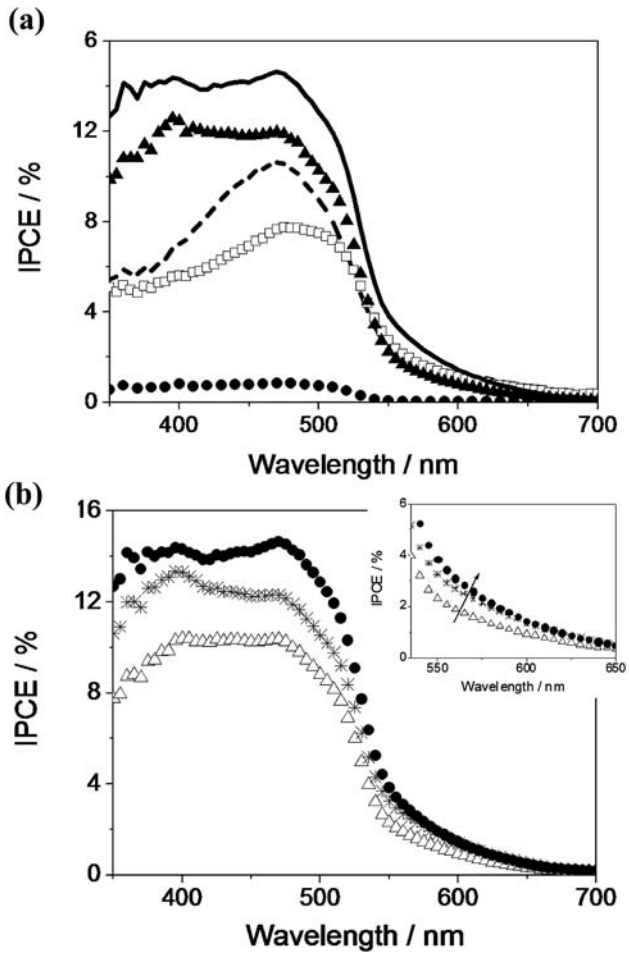

Fig. 4 IPCE curves for devices assembled with 20 wt% of PFT and 80 wt% of PCBM and/or CdSe (4.0 nm), (a) with different concentrations: (---) 1 : 0, (□) 0.7 : 0.3, (—) 1 : 1, (▲) 0.3 : 0.7 e (●) 0 : 1 wt% PCBM : CdSe ratios; or (b) keeping the same concentration (1 : 1 wt% CdSe : PCBM ratio) using different sized CdSe nanoparticles: (△) 2.0 nm, (*) 3.0 nm or (●) 4.0 nm. The inset in (b) shows the magnification of the IPCE curves in the region 550–650 nm, where the contribution of the different sized CdSe nanoparticles can be seen.

band in the region of 550–600 nm (corresponding to the lowest energy excitonic transition) was not observed in the IPCE of any sample. In previous studies, a well-defined peak in IPCE of devices assembled with CdSe nanorods and tetrapods and MDMO-PPV, attributed to the CdSe contribution, was found.[8] On the other hand, other authors also observed only a discrete change in IPCE for devices assembled with CdSe and the same polymer or P3HT.[11] The non observation of a well-defined peak from CdSe contribution in the long-wavelength region in IPCE may suggest that these nanoparticles do not contribute effectively in photovoltaic conversion of light.

However, a more careful analysis of two different regions in the IPCE curves is necessary: (i) the region between 350 to 450 nm, and (ii) the region above 550 nm. In region (ii), where a defined peak arising from direct CdSe contributions would be expected, we can in fact observe a discrete increase in the IPCE values. One must consider this a possible CdSe contribution, even if minimal. In region (i), on the other hand, there are significant changes not only in IPCE values, but also in the curve profile: note that for samples containing only PFT/PCBM or low concentrations of CdSe the IPCE values tend to decay from 450 nm to 350 nm; for the samples with high concentration of CdSe the IPCE values in the same wavelength region remain almost constant, originating a plateau. In this region, the nanoparticles also absorb a significant fraction of light (see the absorption spectra of 4.0 nm sized nanoparticles in Fig. 1).

To further investigate these systems, the IPCE of solar cells assembled with the ternary mixtures, keeping the CdSe : PCBM ratio constant (1 : 1 wt%) and using nanoparticles with different sizes were obtained (Fig. 4b). The different sized CdSe nanoparticles have different absorption properties, as shown in Fig. 1. The inset in Fig. 4b shows that, again, only a discrete increase in IPCE is observed in the region above 550 nm, despite the fact that the smaller nanoparticles (2.0 nm) do not show any light absorption in this region. On the other hand, the formation of a plateau in the region below 450 nm is again observed, also attributed to the nanoparticles effect. It is also interesting to note that the IPCE values increase as the nanoparticle size increases. According to Greenham *et al.*,[17] keeping the concentration of CdSe in the film constant, higher efficiencies are obtained when using larger nanoparticles. The authors did not attribute this improvement to the enhanced light absorption properties of larger nanoparticles, but to a morphology effect: for the same CdSe concentration, the percolation network originated in the film is more effective for larger nanoparticles than for smaller nanoparticles, which contributes to a more efficient charge transport.

Although we consider the change in IPCE profile after incorporation of CdSe as a possible result from light absorption contributions from these nanoparticles, we can not discard morphology effects.

Fig. 5 shows the absorption properties of films made of PFT/CdSe, PFT/PCBM or PFT/CdSe/PCBM. These results show that, after mixing the nanoparticles with the polymer, or polymer and PCBM, the characteristic lowest energy excitonic transition is not clearly seen, as is the case for the nanoparticles in solution (Fig. 1). In the literature it is shown that thin films of CdSe with crystallite sizes of 13 nm already present a tail in the 550 to 800 nm region, showing similar characteristics to bulk CdSe.[38]

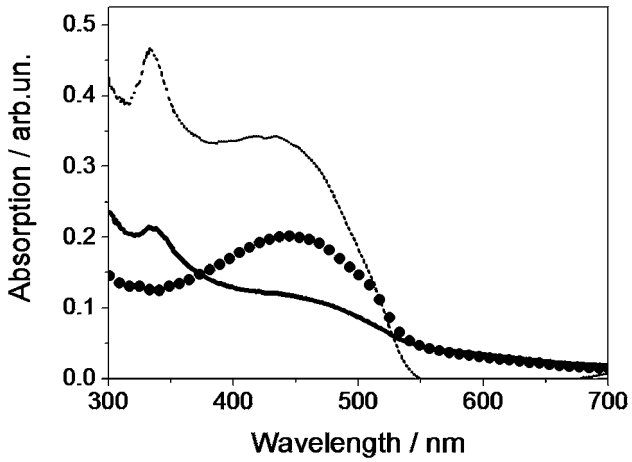

Fig. 5 Absorption spectra of films containing 20 wt% of PFT and (---) 80 wt% of PCBM, (●) 80 wt% of CdSe and (—) 40 wt% of PCBM + 40 wt% of CdSe. The nanoparticle used have preferential diameter sizes of 4.0 nm.

Thus, we could expect that in our systems, the 4.0 nm sized nanoparticles form agglomerates similar to this.

Fig. 6 shows HRTEM images of pure CdSe nanoparticles (preferential diameter = 4.0 nm as estimated with eqn (1)), and the ternary systems based on PFT/CdSe/PCBM, with different

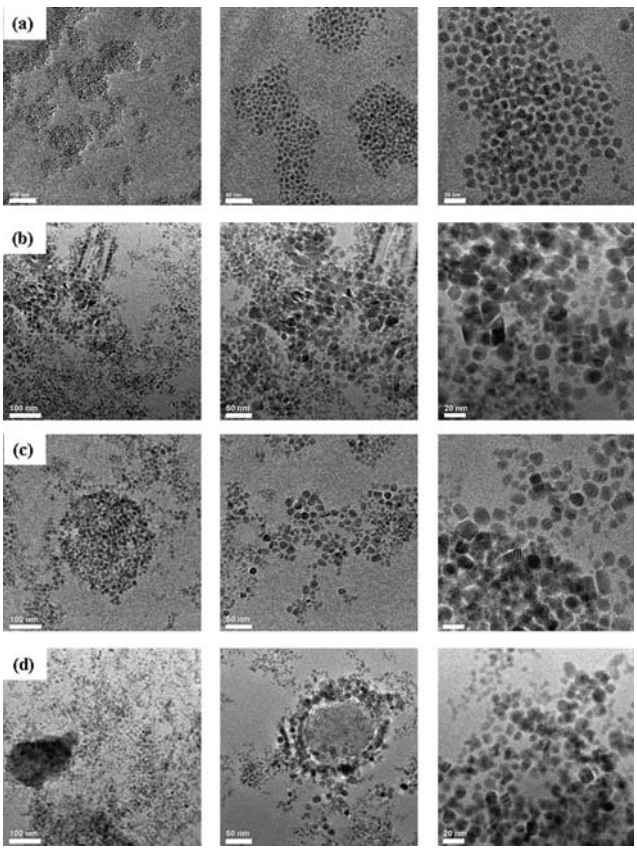

Fig. 6 HRTEM obtained for (a) pure CdSe nanoparticles (preferential diameter of 4.0 nm, as estimated using eqn (1)), and the ternary system PFT/PCBM/CdSe, with different concentrations: (b) 0.3 : 0.7, (c) 1 : 1 or (d) 0.7 : 0.3 wt% PCBM : CdSe ratio. The scale bar indicates 100 nm (left), 50 nm (centre) or 20 nm (right).

CdSe : PCBM ratios, keeping the concentration of polymer constant, at 20 wt%. For the pure CdSe sample, nanoparticles with diameters varying from 3.0 to 9.0 nm can be found (see histogram in Fig. 1). In the ternary mixtures, the nanoparticles show larger sizes, with diameters varying between ~13 to 15 nm, reaching 20 nm in the sample prepared with the higher concentration of CdSe (Fig. 6b). These results show that, once the film is deposited, the CdSe nanoparticles aggregate to form larger structures, which probably have absorption characteristics similar to the solid bulk, losing the characteristic, well-defined, excitonic transition band. This may explain why a tail is observed instead of a defined peak in the longer-wavelength region in the IPCE curves for the ternary system-based solar cells.

Chen *et al.*[36] reported recently that the incorporation of CdTe nanoparticles in films of P3HT/PCBM changes the *J–V* characteristics of the devices. These authors also observed only a discrete increase in absorption in wavelengths longer than 650 nm and shorter than 450 nm for films of P3HT/PCBM/CdTe after the addition of the nanoparticles, and the formation of highly condensed aggregates of CdTe in the film, as observed by HRTEM.

Fig. 7 shows the AFM images obtained for films of PFT/PCBM, PFT/CdSe, and ternary mixtures PFT/PCBM/CdSe containing different amounts of nanoparticles and fullerene. The polymer concentration is kept constant (20 wt%) in all samples. The results show that the morphology of the PFT/PCBM system is very smooth, while for the sample composed of PFT/CdSe and the ternary mixtures it is much rougher, especially for higher concentrations of CdSe. The nanoscale morphology is a crucial parameter, since the effectiveness of the interface for exciton splitting into free charge carriers, and the formation of a percolation network for efficient transport of charge carriers to the electrodes depend on that. It has been shown for P3HT/PCBM- and MDMO-PPV/PCBM-based devices that grain size, roughness and phase separation must be controlled/optimized in order to improve the efficiency of devices.[39–41]

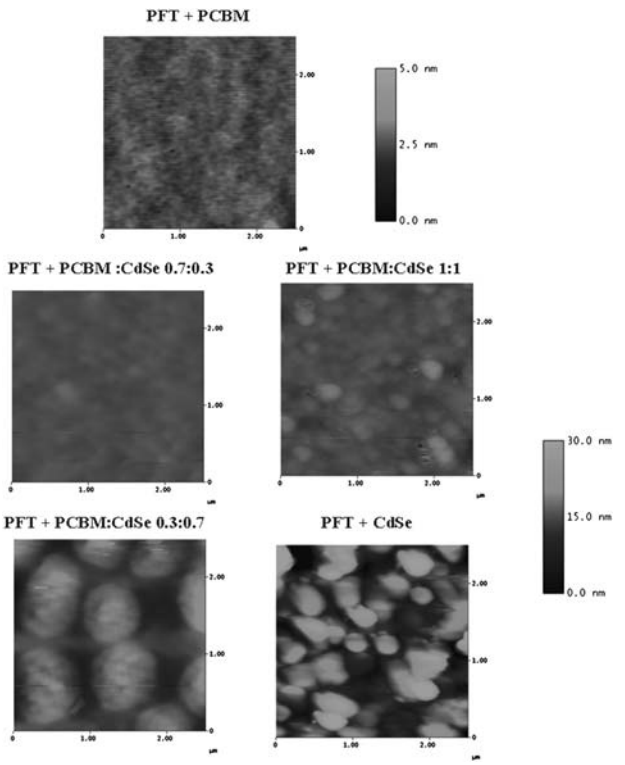

Fig. 7 AFM images obtained in the tapping mode for films of PFT containing 80 wt% of PCBM and/or CdSe, deposited onto PEDOT : PSS covered ITO-glass substrates. The nanoparticles used have 4.0 nm size. The scan area is 2.5 μm × 2.5 μm for all samples. The scale indicates 5 nm for the PFT/PCBM sample, and 30 nm for the ternary mixtures and the PFT/CdSe sample.

To further investigate this morphology effect, films of PFT/PCBM/CdSe with 1 : 1 wt% ratio CdSe : PCBM, with nanoparticles of different sizes, were also analyzed by AFM (Fig. 8). The images obtained show that, for each different nanoparticle size, the morphology changes drastically, despite the fact that the same material concentrations are used. In this case, the morphology effect might also explain the differences observed in IPCE when nanoparticles of different sizes are used, as seen in Fig. 4b (note that if the morphology was the same independent of the CdSe size, the differences in IPCE would have to come essentially from differences in light absorption).

The morphology effect is also seen in the optical microscopy images of the films prepared with different concentrations of CdSe and PCBM. For the binary system, polymer/PCBM, or the ternary mixture with higher PCBM concentration, dark-colored particles can be seen (see Fig. S3 in the ESI†). They are attributed to PCBM-rich domains and, according to Troshin *et al.*,[42] for films made of P3HT and fullerene derivatives the existence of these agglomerates suggests a pronounced phase separation during film formation, related to the solubility of the materials in the solvent used. According to these authors, the morphology is optimized when the solubility of the polymer and the fullerene derivative in the chosen solvent are similar.

Is the TOPO alone responsible for these morphology changes? To answer this question, new solar cells were assembled containing PFT, PCBM and different amounts of pure TOPO, instead of the previously used TOPO-capped CdSe nanoparticles. The results obtained show that when pure TOPO is added the solar cells present an ohmic behavior instead of the

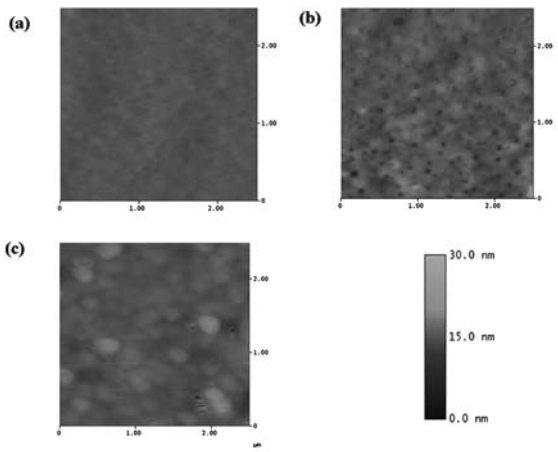

Fig. 8 AFM images obtained in the tapping mode for films of PFT containing 80 wt% of PCBM + CdSe (1 : 1 wt% ratio) using inorganic nanoparticles with different sizes: (a) 2.0 nm, (b) 3.0 nm or (c) 4.0 nm. The scan area is 2.5 μm × 2.5 μm for all samples. The scale bar indicates 30 nm.

expected diode behavior, independent of the amount of TOPO, (see Fig. S4 in the ESI†). Therefore, we concluded that TOPO alone, at least in the free form, must behave as an insulator, and is not responsible for the improvements in device performance.

In any case, considering that the best device has 40 wt% of CdSe added to the mixture of PFT (20 wt%) and PCBM (40 wt%), this amount is too high to be an inert, inactive part of the bulk-heterojunction. In the case of P3HT/PCBM devices with alkylthiol additives,[43,44] for example, the insulator molecules added to improve morphology are usually removed during the vacuum process used to dry the films, and their presence is almost undetectable in the film after that, as reported by Peet *et al.*[45] Thus, we consider that the CdSe nanoparticles must also act with other mechanisms to improve device performance.

Solar cells were also assembled with PFT/CdSe/PCBM with different concentrations using different sized CdSe nanoparticles (see Fig. S5 in the ESI†). An increase in V_{oc} values is systematically observed as the concentration of CdSe increases, related to the LUMO increase of CdSe in comparison with PCBM, as discussed before. When keeping the same concentration of materials in the devices, the J_{sc} increases with increasing CdSe size, the same trend as in IPCE in Fig. 4b. This may be attributed both to better light-harvesting and to the more pronounced morphology effect observed when using larger nanoparticles. Interestingly, the J_{sc} values are significantly higher for the CdSe : PCBM 1 : 1 wt% ratio, independent of the nanoparticle size. At this condition there must be a balance between the effects of CdSe incorporation and charge transport in the PCBM phase.

From the results obtained it is evident that the incorporation of CdSe nanoparticles in the mixture PFT/PCBM improves the device performance. To further investigate this, and see if this improvement is also valid for other systems, new devices were assembled with the ternary mixture, keeping the PCBM : CdSe ratio constant (1 : 1 wt% ratio) and changing the polymer. The copolymer poly[(9,9-dihexyl-9*H*-fluorene-2,7-diyl)-1,2-ethenediyl-1,4-phenylene-1,2-ethenediyl]-*co*-[(9,9-dihexyl-9*H*-fluorene-2,7-diyl)-1,2-ethenediyl-2,5-thiophene-1,2-ethenediyl] (PF-PFT) was used. This material was investigated and characterized in solar cells assembled with PCBM, and presented better performance when compared to PFT, which was related, among other factors, to the higher molar mass of this material.[13] The *J–V* curves obtained with the different polymers and CdSe/PCBM are shown in Fig. 9.

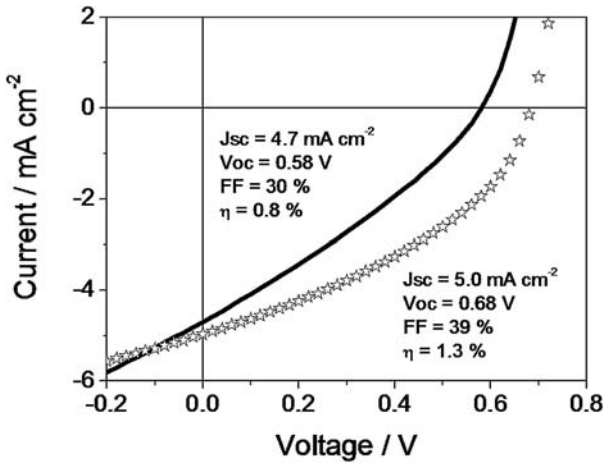

Fig. 9 *J–V* curves for photovoltaic cells illuminated at 100 mW cm^{-2} (active area ≈ 0.1 cm^2), assembled with polymer/PCBM/CdSe (1 : 1 wt% PCBM : CdSe ratio, for nanoparticles with preferential diameter of 4.0 nm), using different polymers: (—) PFT or (☆) PF-PFT. The parameters extracted from the curves are shown.

The J_{sc}, V_{oc}, FF and efficiency values are shown in Fig. 9. The use of the PF-PFT copolymer slightly improves J_{sc}, but significantly improves V_{oc} and FF. The V_{oc} is increased because the HOMO of PF-PFT (−5.6 eV) is shifted to more negative values in comparison to PFT (−5.4 eV).[13] The improvement in FF is expected to be related to a better morphology when using this material, originated from a more favorable interaction of PF-PFT with CdSe and/or PCBM, solubility effects, or due to the higher molar mass observed for this copolymer.[13] The efficiency obtained with both polymers (0.8% for PFT and 1.3% for PF-PFT at 100 mW cm^{-2}) are very promising, especially considering that important parameters such as film thickness were not optimized in this study. We consider that the results presented here indicate that this approach may possibly be extended to other polymers and fullerenes, and show the potential of these new ternary, hybrid systems. The addition of CdSe, as well as other types of inorganic nanoparticles to P3HT/PCBM bulk-heterojunction solar cells is currently under investigation in our laboratory.

Conclusions

In this work, the effect of CdSe incorporation in a polymer/PCBM system was systematically investigated. From the results it was evident that the incorporation of CdSe nanoparticles in the mixture PFT/PCBM changes the film morphology, and this (at least partially) is responsible for the improvement in device photocurrent and efficiency. On the other hand, one must also consider the contribution in light absorption, originated from the larger nanoparticle aggregates formed in the films, even if this effect is less pronounced than the morphology effect. This approach can be extended to other systems, with other polymers, for example. The incorporation of CdSe and other inorganic nanoparticles in P3HT/PCBM bulk heterojunction solar cells is currently underway in our laboratory. The use of nanoparticles capped with other materials than TOPO should also be an interesting option to further improve these ternary systems.

Acknowledgements

The authors thank LME/LNLS for the HRTEM images, and CNPq and Fapesp (fellowship 05/56924-0) for financial support. We also thank Prof. Carol Collins for English revision.

Notes and references

1 B. R. Saunders and M. L. Turner, *Adv. Colloid Interface Sci.*, 2008, **138**, 1.
2 E. Arici, D. Meissner, F. Schaffler and N. S. Sariciftci, *Int. J. Photoenergy*, 2003, **5**, 199.
3 E. Arici, N. S. Sariciftci and D. Meissner, *Adv. Funct. Mater.*, 2003, **13**, 165.
4 W. U. Huynh, J. J. Dittmer and A. P. Alivisatos, *Science*, 2002, **295**, 2425.
5 W. U. Huynh, J. J. Dittmer, W. C. Libby, G. L. Whiting and A. P. Alivisatos, *Adv. Funct. Mater.*, 2003, **13**, 73.

6 L. Han, D. Qin, X. Jiang, Y. Liu, L. Wang, J. Chen and Y. Cao, *Nanotechnology*, 2006, **17**, 4736.
7 Y. Zhou, Y. Li, H. Zhong, J. Hou, Y. Ding, C. Yang and Y. Li, *Nanotechnology*, 2006, **17**, 4041.
8 B. Sun, E. Marx and N. C. Greenham, *Nano Lett.*, 2003, **3**, 961.
9 I. Gur, N. A. Fromer, C.-P. Chen, A. G. Kanaras and A. P. Alivisatos, *Nano Lett.*, 2007, **7**, 409.
10 B. Sun, H. J. Snaith, A. S. Dhoot, S. Westenhoff and N. C. Greenham, *J. Appl. Phys.*, 2005, **97**, 014914.
11 S.-H. Choi, H. Song, I. K. Park, J.-H. Yum, S.-S. Kim, S. Lee and Y.-E. Sung, *J. Photochem. Photobiol., A*, 2006, **179**, 135.
12 A.-W. Tang, F. Teng, H. Jui, Y.-H. Gao, Y.-B. Hou, C.-J. Liang and Y.-S. Wang, *Mater. Lett.*, 2007, **61**, 2178.
13 J. N. de Freitas, A. Pivrikas, B. F. Nowacki, L. C. Akcelrud, N. S. Sariciftci, A. F. Nogueira, *Synth. Met.*, submitted.
14 Z. A. Peng and X. G. Peng, *J. Am. Chem. Soc.*, 2001, **123**, 1389.
15 W. W. Yu, L. H. Qu, W. Z. Guo and X. G. Peng, *Chem. Mater.*, 2003, **15**, 2854.
16 J. Liu, T. Tanaka, K. Sivula, A. P. Alivisatos and J. M. J. Fréchet, *J. Am. Chem. Soc.*, 2004, **126**, 6550–6551.
17 N. C. Greenham, X. Peng and A. P. Alivisatos, *Phys. Rev. B: Condens. Matter*, 1996, **54**, 17628.
18 C. J. Brabec, A. Cravino, D. Meissner, N. S. Sariciftci, T. Fromherz, M. T. Rispens, L. Sanchez and J. C. Hummelen, *Adv. Funct. Mater.*, 2001, **11**, 374.
19 Y.-Y. Lin, C.-W. Chen, J. Chang, T. Y. Lin, I. S. Liu and W.-F. Su, *Nanotechnology*, 2006, **17**, 1260.
20 P. Wang, A. Abrusci, H. M. P. Wong, M. Svensson, M. R. Andersson and N. C. Greenham, *Nano Lett.*, 2006, **6**, 1789.
21 D. S. Ginger and N. C. Greenham, *Synth. Met.*, 1999, **101**, 425.
22 D. S. Ginger and N. C. Greenham, *Phys. Rev. B: Condens. Matter Mater. Phys.*, 1999, **59**, 10622.
23 E. Kucur, J. Riegler, G. Urban and T. Nann, *J. Chem. Phys.*, 2004, **121**, 1074.
24 J. Robel, M. Kuno and P. V. Kamat, *J. Am. Chem. Soc.*, 2007, **129**, 4136.
25 A. Kongkanand, K. Tvrdy, K. Takechi, M. Kuno and P. V. Kamat, *J. Am. Chem. Soc.*, 2008, **130**, 4007.
26 P. V. Kamat, *J. Phys. Chem. C*, 2008, **112**, 18737.
27 D. R. Baker and P. V. Kamat, *Adv. Funct. Mater.*, 2009, **19**, 805.
28 S. W. Tong, C. F. Zhang, C. Y. Jiang, G. Liu, Q. D. Ling, E. T. Kang, D. S. H. Chan and C. Zhu, *Chem. Phys. Lett.*, 2008, **453**, 73.
29 F.-C. Chen, J.-L. Wu, C.-L. Lee, Y. Hong, C.-H. Kuo and M. H. Huang, *Appl. Phys. Lett.*, 2009, **95**, 013305.
30 J. H. Lee, J. H. Park, J. S. Kim, D. Y. Lee and K. Cho, *Org. Electron.*, 2009, **10**, 416.
31 D. Duche, P. Torchio, L. Escoubas, F. Monestier, J.-J. Simon, F. Flory and G. Mathian, *Sol. Energy Mater. Sol. Cells*, 2009, **93**, 1377.
32 H.-Y. Chen, M. K. F. Lo, G. Yang, H. G. Monbouquette and Y. Yang, *Nat. Nanotechnol.*, 2008, **3**, 543.
33 B. V. K. Naidu, J. S. Park, S. C. Kim, S.-M. Park, E.-J. Lee, K.-J. Yoon, S. J. Lee, J. W. Lee, Y.-0S. Gal and S.-H. Jin, *Sol. Energy Mater. Sol. Cells*, 2008, **92**, 397.
34 A. J. Morfa, K. L. Rowlen, T. H. Reilly III, M. J. Romero and J. van de Lagemaat, *Appl. Phys. Lett.*, 2008, **92**, 013504.
35 M. Park, B. D. Chin, J.-W. Yu, M.-S. Chun and S.-H. Han, *J. Ind. Eng. Chem.*, 2008, **14**, 382.
36 M. Y. Chang, Y. F. Chen, Y. S. Tsai and K. M. Chi, *J. Electrochem. Soc.*, 2009, **156**, B234.
37 A. Biebiersdorf, R. Dietmuller, A. S. Susha, A. L. Rogach, S. K. Poznyak, D. V. Talapin, H. Weller, T. A. Klar and J. Feldmann, *Nano Lett.*, 2006, **6**, 1559.
38 K. R. Murali, V. Swaminathan and D. C. Trivedi, *Sol. Energy Mater. Sol. Cells*, 2004, **81**, 113.
39 H. Hoppe, M. Niggemann, C. Winder, J. Kraut, R. Hiesgen, A. Hinsch, D. Meissner and N. S. Sariciftci, *Adv. Funct. Mater.*, 2004, **14**, 1005.
40 X. Yang, J. Loos, S. C. Veenstra, W. J. H. Verhees, M. M. Wienk, J. M. Kroon, M. A. J. Michels and R. A. J. Janssen, *Nano. Lett.*, 2005, **5**, 579.
41 H. Hoppe and N. S. Sariciftci, *J. Mater. Chem.*, 2006, **16**, 45.
42 P. A. Troshin, H. Hoppe, J. Renz, M. Egginger, J. Y. Mayorova, A. E. Goryachev, A. S. Peregudov, R. N. Lyubovskaya, G. Gobsch, N. S. Sariciftci and V. F. Razumov, *Adv. Funct. Mater.*, 2009, **19**, 779.
43 A. Pivrikas, P. Stadler, H. Neugebauer and N. S. Sariciftci, *Org. Electron.*, 2008, **9**, 775.
44 J. Peet, C. Soci, R. C. Coffin, T. Q. Nguyen, A. Mikhailovsky, D. Moses and G. C. Bazan, *Appl. Phys. Lett.*, 2006, **89**, 252105.
45 J. Peet, J. Y. Kim, N. E. Coates, W. L. Ma, D. Moses, A. J. Heeger and G. C. Bazan, *Nat. Mater.*, 2007, **6**, 497.